Characterization of the Structural and Electronic Properties of Crystalline Lithium Silicates

Jincheng Du and L. René Corrales*

Chemical Science Division, Pacific Northwest National Laboratory, Richland, Washington 99352

Received: November 27, 2005; In Final Form: April 12, 2006

Density functional theory (DFT) calculations within the generalized gradient approximation (GGA) were performed to study the atomic and electronic structure of lithium silicate crystals that were fully optimized within the theory. It is found that the relative stability of two crystalline forms of lithium disilicate agrees well with experimental results. The calculated electronic density of states shows distinguishable contributions to the oxygen 2s and upper valence bands associated with bridging (BO) and nonbridging oxygen (NBO) atoms. Bond ionicity, characterized by determining the relative atomic charges, is used to distinguish BO and NBO atoms as well as the corresponding Si−BO and Si−NBO bonds. Results from this work reveal that atomic charges obtained by using population analysis methods based on electron deformation density rather than total electron density provide an accurate description of bond ionicity consistent with chemical intuition.

1. Introduction

Characterization of the electronic structure and the nature of chemical bonds in materials can lead to a better understanding of structure−property relationships useful in the design and fabrication of materials that possess desirable properties. Structure−property relationships of materials are fundamentally determined by the stability of chemical bonds that can be characterized by the degree of ionicity. In principle, atomic charge provides a means to characterize the degree of ionicity of a bond. In silicates, based on Pauling's definition,[1] the silicon−oxygen bonds are considered to be of half covalent and half ionic character. What is desirable is a more descriptive representation of atomic charges that can be used to discriminate the local bond environment in detail.

Silicates are the most abundant and most complicated class of minerals on earth[2] that have tremendous technological applications in such fields as catalysis, microelectronics, biomedicine, photonics, and traditional glass and ceramic industries.[2,3] In particular, the crystalline lithium silicates are present as important phases in silicate glass-ceramics[4] and are promising candidate materials for solid-state electrolyte Li batteries[5] and tritium breeder materials in fusion reactors.[6,7] The structural information of the lithium silicate crystals also serves as reference models for related lithium silicate glasses. The purpose of this work is to theoretically determine the atomic and electronic structures of several important lithium silicate crystals that can be used to ascertain the quality of modern theoretical charge analysis methods.

It is well-known that atomic charges cannot be uniquely determined by using ab initio methods where their values depend on the methods chosen to partition quantities such as electron density.[8] The most commonly used charge analysis method, namely the Mulliken population analysis, assigns charges to a specific atom based on all the basis functions centered on that atom position.[9] Furthermore, the Mulliken charges do not converge with increasing basis set sizes and the charges show strong basis set dependence.[8] Another class of charge analysis method is based on the electron density instead of the molecular orbital (basis functions). Bader[10] and Hirshfeld[11] population analyses belong to this category and have an added advantage that they can be used for plane wave based calculations where the electron density can be directly obtained. Comparison of the atomic charges obtained from different population analysis methods, including the Mulliken, Hirshfeld, and Bader methods, has been made on a number of small molecules[12] and silicate cluster models that represent the bulk materials.[8] It has been shown that Bader and Hirshfeld charges can reproduce the changes of molecular structure and other properties such as electrostatic potentials. The chemical bonds in the small molecules are in general highly covalent in nature and do not provide insight into the behavior of these methods to a system with mixed ionic/covalent character.

Here we provide a systematic study of atomic charges from electron density based population analysis methods in complex lithium silicate crystals where the chemical bonds have high ionic nature. We use known crystal chemistry of lithium silicates to judge the applicability of different charge analysis methods in these silicate crystals. The results show that the charge analysis methods based on electron deformation density (such as the Hirshfeld method) are preferred over those based on total density analysis (such as the standard Bader analysis) where the former better represents the bond ionicity in silicates.

There are only limited reports in the literature on the electronic structure of crystalline lithium silicates. The electronic structure of lithium metasilicate (Li_2SiO_3) and lithium disilicate ($Li_2Si_2O_5$) was calculated by using the orthogonalized linear combination of atomic orbital (OLCAO) method.[13] The calculated partial electronic densities of states were compared with the results of related sodium silicate crystals from similar calculations and it was found that the splitting of the oxygen 2s band is smaller in the lithium cases.[13,14] Atomic charges, obtained by using the Mulliken population analysis, for lithium metasilicate were 0.93 for lithium, 1.39 for silicon, and −1.43 and −1.52 for BO and NBO, respectively.[13] These electronic structure calculations used the experimental crystal structures

* Address correspondence to this author. E-mail: lrcorral@email.arizona.edu. Current address: Departments of Materials Science and Engineering and of Chemistry, The University of Arizona, Tucson, AZ 85721.

10.1021/jp056879s CCC: $33.50
Published on Web 10/14/2006

and the geometries were not optimized.[13,14] The electronic structure of the lithium orthosilicate (Li_4SiO_4) crystal was studied by using the linear combination of atomic orbital (LCAO) Hartree−Fock method with Gaussian basis sets.[7] Electron transfer from lithium and silicon to oxygen ions was visually confirmed from the electron density maps, as well as from atomic charges from Mulliken charge analysis.[7] The Mulliken charges were 1.343−1.435 for silicon, 0.881−0.913 for lithium, and from −1.151 to −1.307 for oxygen. Molecular orbital calculations for small clusters were also performed to study the atomic and electronic structure of lithium silicate glass[15] and hydrogen release on a lithium orthosilicate surface.[6,16]

The crystal structures of lithium metasilicate (Li_2SiO_3) and lithium disilicate ($Li_2Si_2O_5$) have been determined experimentally.[17−19] The orthorhombic Li_2SiO_3 structure has a space group of $Cmc2_1$ with four formula units comprised of 24 atoms per unit cell, with the lattice parameters *a*, *b*, and *c* being 9.392 Å, 5.397 Å, and 4.660 Å.[19] The Li_2SiO_3 structure is comprised of corner sharing [SiO_4] tetrahedra forming parallel chains along the *c*-axis with decorating lithium ions between the chains. Lithium ions are coordinated by four oxygen ions and the Li_2SiO_3 structure can be considered as a framework of corner-sharing [LiO_4] and [SiO_4] tetrahedra with the topology of wurtzite.[19] The monoclinic $Li_2Si_2O_5$ structure has a space group of *Cc* but with strong orthorhombic pseudosymmetry *Ccc*2.[17] The lattice parameter *a*, *b*, and *c* are 5.82 Å, 14.66 Å, and 4.79 Å, respectively, with the unit cell composed of four formula units and a total of 36 atoms. The $Li_2Si_2O_5$ structure consists of layers of [SiO_4] network, with three bridging oxygens per [SiO_4] tetrahedron. Lithium ions are also four-coordinated by oxygen and occupy regions between the silicon oxygen layers. More recently, a metastable $Li_2Si_2O_5$ orthorhombic structure with a space group of *Pbcn* with unit cell parameters of 5.683 Å, 4.784 Å, and 14.648 Å with each unit cell containing four formula units, as in the stable phase, was obtained.[18] The main difference between the metastable $Li_2Si_2O_5$ and the stable form is in the pointing direction of the silicon oxygen tetrahedra within the silicon oxygen layers.[18] The metastable phase was obtained by ion exchange and found to remain stable below 673 K.[18]

In this work, DFT with plane wave basis sets and periodic boundary conditions was used to optimize the atomic structure of several lithium silicate crystals. Mechanical properties, such as the bulk modulus, were determined. The electronic structures including total and partial electronic density of states and atomic charge analyses of these crystals were calculated based on the optimized atomic structures.

2. Simulation Methods

Density functional theory calculations employed the Vienna ab initio simulation package (VASP).[20] The projector augmented wave (PAW)[21] pseudopotentials with Perdew-Wang 91[22] generalized gradient approximation (GGA) exchange and correlation functionals were used for silicon and oxygen. The potential used for lithium treats the semicore 1s electrons as valence electrons. The plane wave energy cutoff was 500 eV and the augmentation charge cutoff was 605 eV. Brillouin zone sampling used meshes generated by the Monkhorst−Pack scheme.[23] Energy convergence was tested on different *k*-point meshes for each crystal type that led, for example, to using a $5 \times 7 \times 9$ mesh for lithium metasilicate.

Total energy minimization employed a conjugate gradient method to optimize the atomic geometry and cell shape for different volumes bracketing the experimental volume. Criteria to terminate an optimization included the energy difference between successive steps being smaller than 10^{-5} eV, and all forces on the atoms being smaller than 0.01 eV/Å.

Atomic charges of the crystals were obtained from the Bader, Hirshfeld, and modified Bader (Bader-D described below) population analysis methods. The Bader (or Atom in Molecule, AIM) method partitions the electron density based on the volume determined by the zero flux surfaces around each nucleus.[10] A recently developed algorithm was used for Bader analysis,[24] where the Bader charge can be expressed as

$$Q_A^{\text{Bader}} = Z_A - \int_{\text{Bader volume}} \rho(r)\, dV \quad (1)$$

in which $\rho(r)$ is the electron density, Z_A is the number of valence electrons of atom A, and Q is the atomic charge. The zero flux surface around a certain nucleus that defines the Bader volume is mathematically expressed as

$$\nabla\rho(r)n = 0 \quad (2)$$

where n is the normal vector with respect to the surface.

In contrast, the Hirshfeld method partitions the electron deformation density instead of the electron density.[11] The electron deformation density is the difference of the molecule (or the crystal) electron density and the promolecule density that is the superposition of the ground-state atomic electron density centered at the position of the nucleus in a molecule (or the crystal). Since the partition of charges among atoms is based on the atomic charge density centered at the position of the nucleus, it is also referred to as the stockholder method. The electron deformation density is then partitioned based on the size of the atomic electron density relative to the promolecule density. The Hirshfeld charge can be expressed as

$$Q_A^{\text{Hirshfeld}} = -\int \frac{\rho_A}{\rho_{\text{promolecule}}} [\rho(r) - \rho_{\text{promolecule}}(r)]\, dV \quad (3)$$

where ρ_A is the atomic electron density of atom A. $\rho_{\text{promolecule}}$ is the promolecule electron density defined as

$$\rho_{\text{promolecule}}(r) = \sum_B \rho_B(r) \quad (4)$$

where ρ_B is the ground-state atomic charge density of atom B with its nucleus located at the position of the corresponding atom in the molecule (or the crystal). The electron deformation density is then expressed as $\rho'(r) = \rho(r) - \rho_{\text{promolecule}}(r)$.

Apart from the fact that the Bader method partitions the electron density and that the Hirschfield method partitions the electron deformation density, they also differ in that the former has a discrete boundary and the latter a diffuse boundary.

It has been found that Bader and Hirshfeld charges led to very different charge values although both methods were proved to well reproduce the differences in structure and other properties of small molecules.[12] Thus, a significant difference of the magnitude of the charges from these two methods is expected.

Here we introduce the Bader population analysis based on the electron deformation density that is denoted as Bader-D. The Bader-D method partitions the electron deformation density $\rho'(r)$ to each nucleus according to the volume determined by the zero flux surfaces surrounding the nucleus. The Bader-D charge is defined as

$$Q_A^{\text{Bader-D}} = -\int_{\text{Bader volume}} [\rho(r) - \rho_{\text{promolecule}}(r)]\, dV \quad (5)$$

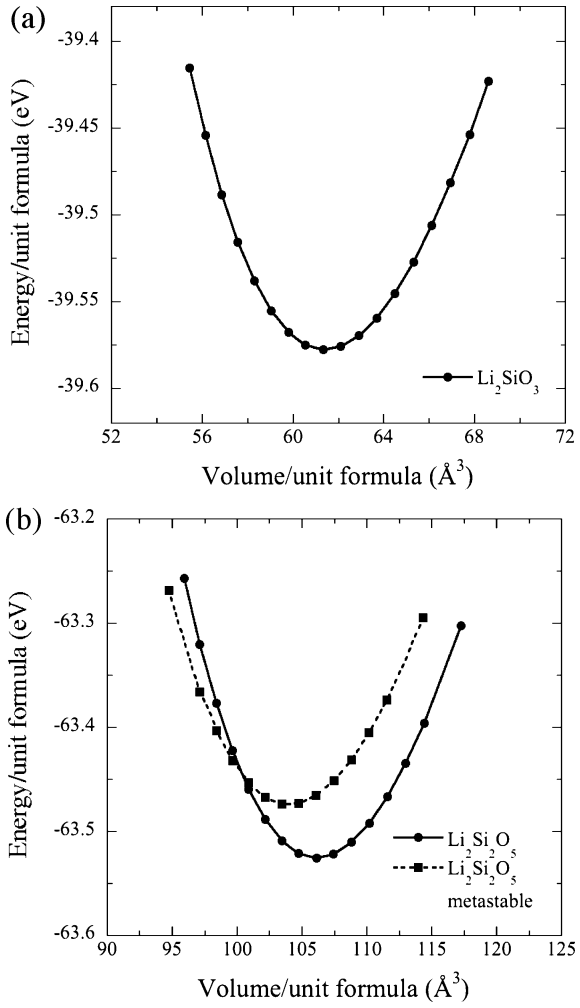

Figure 1. Energy versus volume curves for Li_2SiO_3 (a) and stable (circles) and metastable (squares) $Li_2Si_2O_5$ (b). The data points are from DFT calculations and the curves are fit to the Murnaghan equation of state.[25]

where $\rho(r)$ and $\rho_{\text{promolecule}}$ are defined as above with Q being the atomic charge. The zero flux surface around a certain nucleus that defines the Bader-D volume is

$$\nabla[\rho(r) - \rho_{\text{promolecule}}(r)]n = 0 \qquad (6)$$

similar to eq 2.

3. Results and Discussion

3.1. Structure Optimization. Figure 1 shows the energy versus volume curves for the simulated crystals. The calculated data points show an excellent fit to the Murnaghan equation of state over the whole volume range.[25] Equilibrium volume, energy, bulk modulus, and pressure derivative of the bulk modulus obtained from the fitting are listed in Table 1. The GGA calculation clearly reproduces the relative stability of the stable and metastable form of lithium disilicate crystals. The equilibrium energy of the stable form is 0.05 eV per formula unit (or 0.2 eV per unit cell) less than that of the metastable form. Our calculations also predict that the bulk modulus of stable lithium disilicate (73.4 GPa) is higher than that of the metastable form (66.5 GPa). Previous studies have shown that DFT calculations with GGA correctly predict the relative stability of silica polymorphs while the calculations with LDA do not.[26]

TABLE 1: Calculated Equilibrium Volume, Energy, Bulk Modulus (B), and Its Pressure Derivative (B') of Stable and Metastable $Li_2Si_2O_5$ and Li_2SiO_3 and Available Experimental Data

crystal	method	V_0 (Å^3/uf)[a]	E_o (eV/uf)[a]	B (GPa)	B'
Li_2SiO_3	GGA	61.40	−39.58	72.86	5.12
	expt[19]	59.05			
$Li_2Si_2O_5$	GGA	106.15	−63.52	73.04	4.28
	expt[17]	102.17			
$Li_2Si_2O_5$ (metastable)	GGA	104.00	−63.47	66.48	4.72
	expt[18]	99.63			

[a] uf = unit formula.

The equilibrium volume of the optimized structure is slightly larger than the experimental values: 4.4% for Li_2SiO_3, 3.9% for monoclinic $Li_2Si_2O_5$, and 4.0% for metastable $Li_2Si_2O_5$. This is consistent with observations in silica polymorphs where GGA calculations were found to systematically overestimate the equilibrium volume.[26] As a consequence of this overestimation, the cation−oxygen bond lengths are found to be slightly larger than experimental values. For example, in the optimized Li_2SiO_3 structure, the two silicon−bridging oxygen (BO, oxygen ions bond to two silicon ions) distances are 1.701 and 1.698 Å, respectively, and both the silicon−nonbridging oxygen (NBO, oxygen ions bond to only one silicon ion) distances are 1.609 Å. The corresponding experimental distances are 1.681 and 1.678 Å for Si−BO and 1.592 Å for Si−NBO, with consistent relative differences between the experimental and optimized structures. Similarly, in the optimized structure the three Li−NBO distances are 1.965, 1.962, and 1.996 Å and the Li−BO distance is 2.187 Å, while in the experimental structure the Li−NBO distances are 1.938, 1.937, and 1.955 Å and the Li−BO distance is 2.170 Å. The Si−O−Si bond angle is 124.6° for the optimized Li_2SiO_3 structure as compared to the experimental value of 124.1°.

As in the case of Li_2SiO_3, lithium ions in both monoclinic and metastable $Li_2Si_2O_5$ are also coordinated by four oxygen ions. However, for the monoclinic case, a significant difference between the experimental and optimized theoretical structures is found. In the experimentally determined structure of monoclinic $Li_2Si_2O_5$[17] the lithium site is coordinated by three NBO and one BO, where two of the coordinated oxygen ions, one BO and one NBO, are from the same [SiO_4] tetrahedra. The Li−O bond lengths to these two oxygen ions from the same [SiO_4] tetrahedra are 2.040 and 1.847 Å, for the NBO and BO, respectively, and the other two Li−NBO bond lengths are 1.990 and 1.884 Å. It is rather counterintuitive that the Li−BO has the smallest bond distances among the four Li−O bonds because the general belief is that the cation−NBO distance is shorter than the cation−BO distances.[27] The predicted theoretical structure, however, reverses this trend where structural relaxation leads to a slightly different environment of lithium ions in monoclinic $Li_2Si_2O_5$. In the optimized structure, four oxygen ions consisting of three NBO and one BO are from four different [SiO_4] tetrahedra where the Li−NBO distance is slightly shorter than the Li−BO distance. The Li−NBO distances are 1.987, 1.988, and 1.974 Å, respectively, and the Li−BO distance is 2.084 Å. In the theoretical structure, the Li ion has moved about 0.584 Å away from the position assigned to it in the experimental structure. This shift essentially moves the lithium ion into an adjacent tetrahedron site, and removes the edge-sharing LiO_4 and SiO_4 configuration. One BO and two NBO of the original Li tetrahedron remain while the fourth oxygen is to an adjacent NBO. The bond distance of lithium to this fourth oxygen is originally 2.774 Å (the experimental structure), which shortens to 1.987 Å in the optimized structure.

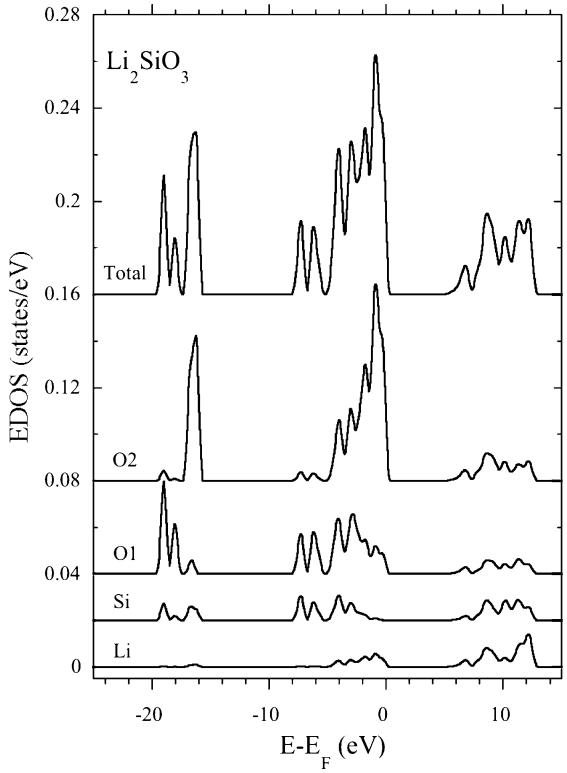

Figure 2. Total and partial electronic density of states of Li_2SiO_3. Spectra were broadened by using a Gaussian function with $\sigma = 0.2$ eV.

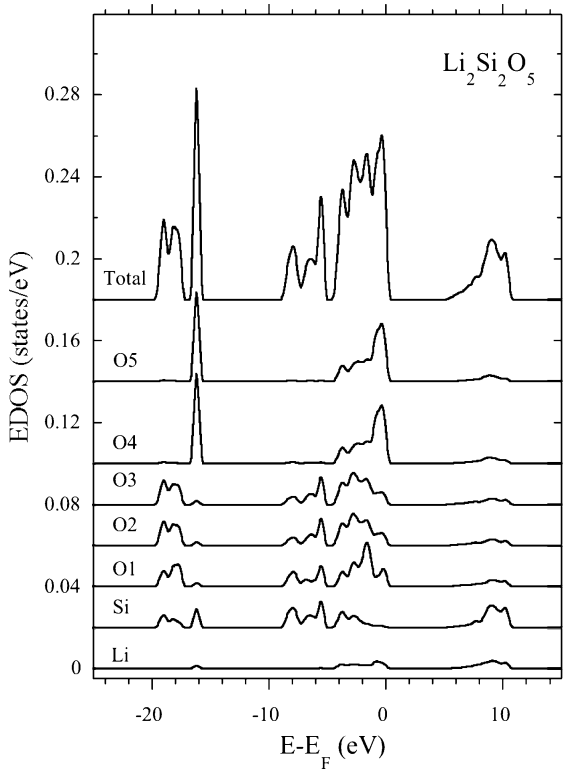

Figure 3. Total and partial electronic density of states of $Li_2Si_2O_5$. Spectra were broadened by using a Gaussian function with $\sigma = 0.2$ eV.

In the metastable $Li_2Si_2O_5$ structure determined more recently,[19] all four oxygen ions coordinating lithium ions are from different [SiO_4] tetrahedra and the Li−NBO distances are found to be slightly shorter than the Li−BO distance. The three Li−NBO distances are 1.943, 2.006, and 2.009 Å and the Li−BO distance is 2.141 Å from the experimental structure.[19] Structural optimization does not change the relative arrangement of atoms around lithium ions but the Li−O bond distances increase slightly to 1.956, 1.996 Å, and 2.040 Å for Li−NBO and 2.095 Å for Li−BO, consistent with the slight increase of the equilibrium volume.

A comparison of the total energy of the optimized and the experimentally determined structure of the monoclinic and metastable $Li_2Si_2O_5$ was made. For the monoclinic structure, it was found that the optimized structure is lower in energy by 0.75 eV per formula unit than that of the original structure. For the metastable structure, the optimized structure is 0.28 eV less in energy than the original form. The larger energy difference in the monoclinic structure is explained by the more stable lithium oxygen tetrahedron in the optimized structure where the configuration of the edge-sharing lithium and silicon oxygen tetrahedron was removed.

3.2. Electronic Structures. *3.2.1. Electronic Density of States.* Calculated total and partial electronic density of states (EDOS) of Li_2SiO_3 are shown in Figure 2. To obtain the partial EDOS, wave functions were projected onto spherical harmonics centered at each atom position and summed over the atoms of the same crystallographic position in each of the unit cells. In addition, the spd projection of each atom was obtained. The calculated EDOS were broadened by using a Gaussian function with a σ of 0.2 eV. The valence band EDOS of Li_2SiO_3 has oxygen 2s bands at −18.9, −18.1, and −16.4 eV, and upper valence bands at −7.3, −6.2, −4.0 , −2.9 , −1.8, and 0.9 eV. The partial EDOS show two specific oxygen sites on the oxygen 2s bands with the −18.9 and −18.1 eV bands being mainly due to BO (O1) while the −16.4 eV band is dominated by NBO (O2) contributions. In the upper valence bands, the near-edge features are mainly due to the oxygen 2p electrons of NBO, while the peaks at −7.3 and −6.2 eV are due to the 2p bonding states of BO and of silicon. Thus, the EDOS features between −10 and −5 eV are due to bonding states between silicon sp^3 hybrid and oxygen 2p orbitals while the highest occupied states consist of oxygen 2p lone pair bands (nonbonding orbitals). The contribution of lithium ions is mainly in the near-edge upper valence band and in the conduction band.

The total and partial EDOS spectra of stable and metastable $Li_2Si_2O_5$ are shown in Figures 3 and 4, respectively. The spectra of $Li_2Si_2O_5$ crystals are very similar to that of Li_2SiO_3 but noticeable differences can be observed on both the O 2s band and upper valence band. The O 2s peaks due to BO and NBO are also separated in $Li_2Si_2O_5$ crystals but the O 2s peak due to NBO (O4 and O5 in $Li_2Si_2O_5$ and O3 in metastable $Li_2Si_2O_5$) at −16.4 eV is considerably sharper than that in Li_2SiO_3. The relative intensity of the O 2s peaks at around −18.9 and −18.1 eV due to BO differs in all three crystals. At the upper valence band, a third peak appears between the −10 and −5 eV bonding states due to the changes of both BO and Si partial EDOS. This can be explained by the fact that each [SiO_4] tetrahedron in Li_2SiO_3 has two BO (Q_2 in the NMR terminology) while each [SiO_4] tetrahedron in $Li_2Si_2O_5$ has three BO (Q_3). This leads to differences of the bonding states between −10 and −5 eV in the Li_2SiO_3 and $Li_2Si_2O_5$ crystals.

The EDOS of lithium silicates obtained in this work have peaks with similar positions as those obtained with OLCAO.[13] In the oxygen 2s bands the peaks associated with the main BO and NBO are separated by 2.8 eV. In general, the spectra obtained in this work show more fine structures than those with OLCAO,[13] although similar broadening of the original EDOS using Gaussian with a σ of 0.2 eV was performed. The BO 2s band in Li_2SiO_3 splits into two major peaks (Figure 2) and the

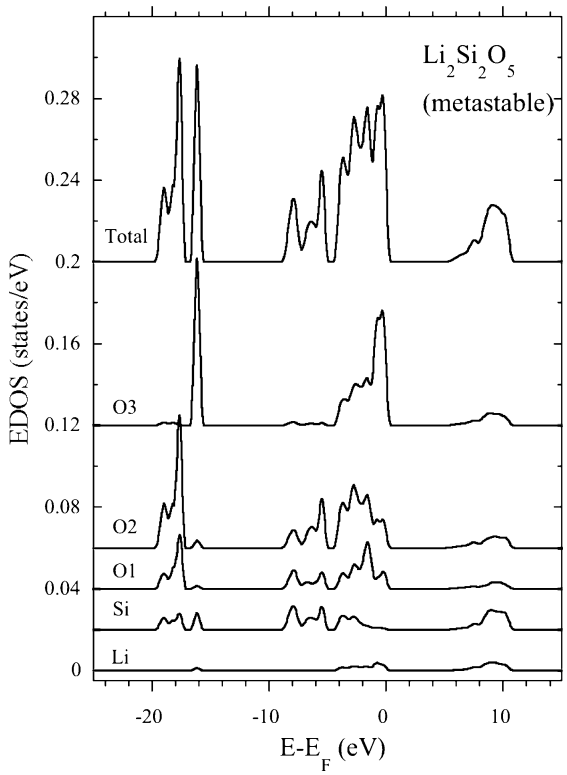

Figure 4. Total and partial electronic density of states of metastable $Li_2Si_2O_5$. Spectra were broadened by using a Gaussian function with $\sigma = 0.2$ eV.

main peak of the BO 2s band is located 2.6 eV lower in energy than the peak position of the single NBO 2s band. A similar splitting of the oxygen (where all oxygens are BO) 2s band in α quartz was observed in previous DFT calculations.[28,29] In the OLCAO calculations, the separation of the BO and NBO 2s band ranging from 1.5 to 2.5 eV was observed for sodium silicates. In contrast, the separation of the BO and NBO 2s band is very small in lithium silicate crystals, which leads to a minimum splitting of oxygen 2s bands in the lithium silicates.[13,14] In the oxygen 2s X-ray absorption spectroscopy (XPS) spectra, both sodium and lithium silicate glass show splitting although the splitting is larger for the sodium silicate glasses.[13] Taking into consideration the inherent experimental broadening of XPS spectra and heterogeneous structural broadening of glasses, a sharp splitting of the oxygen 2s band can be expected for lithium silicate crystals as predicted here.

The band gaps obtained from the EDOS are 5.7 eV for Li_2SiO_3, 5.5 eV for $Li_2Si_2O_5$, and 5.6 eV for metastable $Li_2Si_2O_5$. It is well-known that both LDA and GGA density functional theory calculations systematically underestimate the band gap of insulators and semiconductors.[29,30] It is therefore expected that the band gap values of lithium silicates from our GGA calculations are lower than experimental values. No direct measurement of the optical band gap of lithium silicate is available to the knowledge of the authors. In the linear combination atomic orbital calculations of lithium silicates, the band gap was found to be 7.26 eV for Li_2SiO_3 and 7.45 eV for $Li_2Si_2O_5$.[13]

3.2.2. Atomic Charges. For plane wave basis set calculations, such as used in this work, Mulliken charge analysis cannot be applied directly since plane wave basis sets are generally delocalized. Three alternative charge analysis methods based on the population analysis of electron density, namely the Bader,[10] Hirshfeld,[11] and a modified Bader (Bader-D) analysis, were employed to determine the atomic charges and are compared with each other.

TABLE 2: Atomic Charges of Li_2SiO_3 and Stable and Metastable $Li_2Si_2O_5$ from Bader and Hirshfeld Population Analysis

	Bader	Hirshfeld	Bader-D
Li_2SiO_3			
Li	0.875	0.192	0.253
Si (Q_2)	3.170	0.536	0.568
O1 (BO)	−1.645	−0.195	−0.177
O2 (NBO)	−1.637	−0.363	−0.448
$Li_2Si_2O_5$			
Li1	0.873	0.195	0.228
Li2	0.873	0.195	0.228
Si1 (Q_3)	3.193	0.558	0.550
Si2 (Q_3)	3.194	0.558	0.550
O1 (BO)	−1.635	−0.294	−0.250
O2 (BO)	−1.646	−0.227	−0.193
O3 (BO)	−1.647	−0.227	−0.193
O4 (NBO)	−1.602	−0.378	−0.460
O5 (NBO)	−1.604	−0.378	−0.460
$Li_2Si_2O_5$ (metastable)			
Li	0.875	0.193	0.234
Si (Q_3)	3.195	0.554	0.549
O1 (BO)	−1.652	−0.295	−0.252
O2 (NBO)	−1.606	−0.379	−0.466
O3 (BO)	−1.638	−0.220	−0.191

Atomic charges calculated on the optimized structures are summarized in Table 2. As discussed above, charges obtained by partitioning the electron density are in general larger than the charges obtained by partitioning the electron deformation density. The magnitude and relative differences between Bader and Hirshfeld charges are consistent with previous DFT calculations of zeolite clusters,[8] where the Bader-D charges are consistent with the Hirshfeld charges. For the lithium ion, the Bader charge is around 0.87, the Hirshfeld charge is around 0.19, and the Bader-D charge is around 0.25. With the exception of the Bader-D charge that reduces the charge on Li in going from Li_2SiO_3 to the $Li_2Si_2O_5$ crystals, the other two methods provide essentially the same charge for Li in all three crystals. The silicon Bader charge increases from 3.170 in Li_2SiO_3 to 3.193/3.194 and 3.195 in stable and metastable $Li_2Si_2O_5$, respectively. The Hirshfeld charge of silicon also increases from 0.536 in Li_2SiO_3 to 0.558/0.558 and 0.554 in stable and metastable $Li_2Si_2O_5$, respectively. The Bader-D charge of silicon in contrast decreases from 0.568 in Li_2SiO_3 to 0.550/0.550 and 0.549 in stable and metastable $Li_2Si_2O_5$, respectively. It is possible that a difference in trends of the cations for the Bader-D charges may lie elsewhere in the methods not tested by substituting the electron density with the electron deformation density, thus the origin of this difference is not revealed here. In general, the increase of atomic charges of silicon ions from Q_2 (meaning silicon oxygen tetrahedra with 2 bridging oxygen) in Li_2SiO_3 to Q_3 (silicon oxygen tetrahedra with 3 bridging oxygen) in $Li_2Si_2O_5$ can be explained by the nonlocalized effect of modifier ions,[31] e.g., lithium or sodium, that not only change the chemical environment of their direct neighbors, the oxygen ions, but also affect the environments of silicon ions bonding to these oxygen ions. An increase of positive charge on silicon with increasing n value of Q_n species has also been observed in previous ab initio calculations.[32,33]

The largest differences in trends between the Bader, Hirshfeld, and Bader-D charges show up on the oxygen ions. In Li_2SiO_3, Bader charges are −1.645 on BO and −1.637 on NBO, with the charge on BO being more negative than that of NBO. In contrast, the Hirshfeld charges are −0.195 for BO and −0.363 for NBO, with the charge on NBO being more negative than

that of BO. The Bader-D charges are −0.177 for BO and −0.448 for NBO, with the NBO more negative than the BO. The charges on oxygen in stable and metastable $Li_2Si_2O_5$ follow the same trend: Bader analysis shows more negative charges on BO while Hirshfeld and Bader-D analysis give more negative charges on NBO. Earlier molecular orbital calculations of sodium silicate clusters showed more negative charges on NBO than BO based on Mulliken charge analysis.[32] Intuitively, the NBO should have a more negative charge than BO. The larger difference between the BO and NBO charges observed in the Bader-D methods (in comparison to the Hirschfeld method) coupled with the reduction of charge of the cations with increasing NBO coordination indicates that the Bader-D method assigns greater charge to the NBO thereby excessively removing electron density from the cations.

Both the Bader and Hirshfeld charges obtained in this work are consistent with earlier DFT calculations using localized basis sets based on clusters of silicon−oxygen four-membered rings.[8] The Bader charges of oxygen range from −1.65 to −1.67 and those of silicon range from 3.26 to 3.36.[8] The Hirshfeld charges of oxygen range from −0.26 to −0.32 and those of silicon range from 0.48 to 0.52.[8] All the calculations in ref 8 are based on fragments of fully polymerized Si−O rings and all oxygen ions are BO (all Si are Q^4) in the calculated zeolite cluster.

The obtained atomic charges are used to calculate bond ionicity based on the formula

$$\kappa_{A-B} = \frac{1}{2}\left|\frac{Q_A}{\nu_A} - \frac{Q_B}{\nu_B}\right|$$

in which Q_A and ν_A are the atomic charge and the valence of atom A, respectively.[8,34] In Li_2SiO_3, the bond ionicities calculated from Hirshfeld charges are 0.018 for the Si−BO bond and 0.024 for the Si−NBO bond, consistent with the previous understanding that the Si−NBO bond is more ionic than the Si−BO bond. However, the bond ionicities calculated based on Bader charges are 0.015 for the Si−BO bond and 0.013 for the Si−NBO bond. Consequently, the Bader charges predict higher bond ionicity of the Si−BO bonds. Similarly, the Hirshfeld charges predict higher ionicity of the Si−NBO bonds in stable and metastable $Li_2Si_2O_5$, while the Bader method predicts the reverse trend. The Bader-D charges predict a similar trend as the Hirshfeld charges for all three crystals. In a previous study, the Hirshfeld method was shown to better reproduce the relative ionicity of Si−BO bonds in siliceous materials than the Mulliken and Bader method.[8] It is evident from this work that the Hirshfeld and Bader-D analysis correctly reproduce that the NBO is more negatively charged than BO where the Si−NBO bonds have higher ionicity than the Si−BO bonds. Thus, it becomes apparent that determining charges by partitioning the electron deformation density provides a more accurate description of atomic charge, and therefore ionicity, in systems with mixed ionic and covalent bonding.

The structure of the ambient pressure polymorphs of silica crystals is made up of corner sharing silicon oxygen tetrahedra where all oxygen ions are BO. In alkali silicate crystals, the alkali ions break the Si−O−Si bonds and create NBO. The electron transfer from the alkali ions to the oxygen ions (NBO) leads to more negative charges on NBO than BO, which has been supported by the XPS spectra.[31] A shorter cation−NBO bond length than the cation−BO bond length is expected as predicted by the theoretically determined atomic structures of lithium silicate crystals. The Hirshfeld and Bader-D charges reproduce the charge differences of BO and NBO correctly, while the Bader charges do not. This difference can be traced back to the definition of the Bader versus the Hirshfeld and Bader-D charges. The crystal chemistry of lithium silicate crystals is well understood and the difference of BO and NBO provide a unique opportunity to compare the atomic charges obtained from different methods.

The electron deformation density better reproduces the charges and bond ionicity because such a method captures the flux of charge flow from one nucleus to another upon the formation of the crystal. In more ionic systems, the charge flow from one nucleus to another is more dramatic than the covalent bond where the electrons are shared between atoms. Previous comparisons of the different population analysis methods were mostly performed on small molecules, where the chemical bonds are highly covalent, and therefore such differences as those found in this work would not be expected. However, since the Bader method provides a unique way to assign electron density to a specific nucleus, we anticipated that it could also be used to analyze the electron deformation density. The Bader-D charges were found to have similar magnitude as the Hirshfeld charges and trends, owing to using the same electron deformation density. The results of the Bader-D approach provide strong supportive evidence to our analysis that the electron deformation density is preferred over the total electron density in charge analysis methods in systems containing a mix of ionic and covalent bonding character.

4. Conclusions

Structural and electronic properties of fully optimized lithium silicate crystals were characterized by using DFT within the GGA with the PAW pseudopotentials. It was found that the relative stability of the metastable and stable lithium disilicate is reproduced in DFT GGA calculations, and that the electronic density of states reveals clear differences of the bridging and nonbridging oxygen ions in the 2s valence bands, the bonding states, and the upper valence band. We have shown, through charge analyses, that the atomic charges based on electron deformation density reproduce the charge differences of the BO and NBO species and their relative bond ionicity, consistent with chemical intuition and experiment. This work reveals that the population analysis using the electron deformation density within the Hirshfeld and Bader-D methods is preferred for systems with a mix of ionic and covalent bonding.

Acknowledgment. This work was supported by the Division of Chemical Sciences, Office of Basic Energy Sciences, of the U.S. Department of Energy (DOE). This research was performed in part using the Molecular Science Computing Facility in the William R. Wiley Environmental Molecular Sciences Laboratory (EMSL) at the Pacific Northwest National Laboratory (PNNL). The EMSL is funded by DOE's Office of Biological and Environmental Research. Battelle operates PNNL for DOE.

References and Notes

(1) Pauling, L. *The Nature of the Chemical Bond*; Cornell University Press: Ithaca, New York, 1960.

(2) Liebau, V. F. *Structural Chemistry of Silicates. Structure, Bonding and Classifcation*; Springer-Verlag: New York, T 1985.

(3) Iler, R. K. *The Chemistry of Silica*; Wiley: New York, 1979. Iler, R. K. *Silica Glass and Its Application*; Elsvier, Amsterdam, The Netherlands, 1990.

(4) Beall, G. H. *Annu. Rev. Mater. Sci.* **1992**, *22*, 91.

(5) Vinod, M. P.; Bahnemann, D. *J. Solid State Electrochem.* **2002**, *6*, 498.

(6) Nakazawa, T.; Yokoyama, K.; Noda, K. *J. Nucl. Mater.* **1998**, *258−263* (pt A), 571.

(7) Munakata, K.; Yokoyama, Y. *J. Nucl. Sci. Technol*. **2001**, *38* (10), 915.
(8) Zwijnenburg, M. A.; Bromley, S. T.; Van Alsenoy, C.; Maschmeyer, T. *J. Phys. Chem. A* **2002**, *106*, 12376.
(9) Mulliken, R. S. *J. Chem. Phys*. **1955**, *23*, 1833.
(10) Bader, R. F. W. *Atoms in Molecule−a Quantum Theory*; Oxford University Press: Oxford, U.K., 1990.
(11) Hirshfeld, F. L. *Theor. Chim. Acta* (*Berlin*) **1977**, *44*, 129.
(12) Wiberg, K. B.; Rablen, P. R. *J. Comput. Chem*. **1993**, *14* (12), 1504.
(13) Ching, W. Y.; Li, Y. P.; Veal, B. W.; Lam, D. J. *Phys. Rev. B* **1985**, *32* (2), 1203.
(14) Ching, W. Y.; Murray, R. A.; Lam, D. J.; Veal, B. W. *Phys. Rev. B* **1983**, *28*, 4724.
(15) Uchino, T.; Yoko, T. *J. Phys. Chem. B* **1999**, *103* (11), 1854.
(16) Nakazawa, T.; Yokoyama, K.; Grismanovs, V.; Katano, Y. *J. Nucl. Mater*. **2000**, *279* (2−3), 201.
(17) Liebau, V. F. *Acta Crystallogr*. **1961**, *14*, 389.
(18) Smith, R. I.; Howie, R. A.; West, A. R. *Acta Crystallogr., Sect. C*: *Cryst. Struct. Commun*. **1990**, *46*, 363.
(19) Hesse, H.-F. *Acta Crystallogr. Sect. B*: *Struct. Sci*. **1977**, *33*, 901.
(20) Kresse, G.; Furthmüller, J. *Comput. Mater. Sci*. **1996**, *6*, 15. Kresse, G.; Furthmüller, J. *Phys. Rev. B* **1996**, *54*, 11169.
(21) Kresse, G.; Joubert, J. *Phys. Rev. B* **1996**, *59*, 1758.
(22) Perdew, J. P.; Chevary, J. A.; Vosko, S. H.; Jackson, K. A.; Pederson, M. R.; Singh, D. J.; Fiolhais, C. *Phys. Rev. B* **1992**, *46*, 6671.
(23) Monkhorst, H. J.; Pack, J. D. *Phys. Rev. B* **1976**, *16*, 5188.
(24) Henkelman, G.; Arnaldsson, A.; Jonsson, H. *Comput. Mater. Sci*. In press.
(25) Murnaghan, F. D. *Proc. Natl. Acad. Sci. U.S.A.* **1944**, *30*, 244.
(26) Demuth, T.; Jeanvoine, Y.; Hafner, J.; Angyan, J. G. *J. Phys.*: *Condens. Matter* **1999**, *11*, 3833.
(27) Hill, R. J.; Gibbs, G. V. *Acta Crystallogr., Sect. A*: *Found. Crystallogr*. **1978**, *34*, 127.
(28) Binggeli, N.; Troullier, N.; Martins, J. L.; Chelikowsky, J. R. *Phys. Rev. B* **1991**, *44* (10), 4771.
(29) Sarnthein, J.; Pasquarello, A.; Car, R. *Phys. Rev. B* **1995**, *52* (17), 12690.
(30) Terki, R.; Feraoun, H.; Bertrand, G.; Aourag, H. *Comput. Mater. Sci*. **2005**, *33*, 44.
(31) Bruckner, R.; Chun, H.-U.; Goretzki, H.; Sammet, M. *J. Non-Cryst. Solids* **1980**, *42*, 49.
(32) Uchino, T.; Iwasaki, M.; Sakka, T.; Ogata, Y. *J. Phys. Chem*. **1991**, *95*, 5455.
(33) Uchino, T.; Sakka, T.; Ogata, Y.; Iwasaki, M. *J. Phys. Chem*. **1993**, *97*, 9642.
(34) Chulviken, N. D.; Zhidomirov, V. B. *Kinet. Katal*. **1977**, *18*, 903.